

In situ synchrotron x-ray diffraction studies monitoring mechanochemical reactions of hard materials: Challenges and limitations

Cite as: Rev. Sci. Instrum. **92**, 114102 (2021); <https://doi.org/10.1063/5.0068627>

Submitted: 26 August 2021 • Accepted: 26 October 2021 • Published Online: 08 November 2021

 Tobias Rathmann, Hilke Petersen, Steffen Reichle, et al.



View Online



Export Citation



CrossMark

ARTICLES YOU MAY BE INTERESTED IN

[A femtosecond magnetic circular dichroism spectrometer](#)

Review of Scientific Instruments **92**, 113001 (2021); <https://doi.org/10.1063/5.0064460>

[Fast and direct optical dispersion estimation for ultrafast laser pulse compression](#)

Review of Scientific Instruments **92**, 113702 (2021); <https://doi.org/10.1063/5.0060564>

[On the robustness of model-based algorithms for photoacoustic tomography: Comparison between time and frequency domains](#)

Review of Scientific Instruments **92**, 114901 (2021); <https://doi.org/10.1063/5.0065966>



www.amscins.com

3D IMAGING of Ions & Electrons

Perfect replacement for conventional 2D cameras

TPX3CAM READOUT			
TIME OF FLIGHT EXPERIMENT		29.05.2021	
ToA (sec)	ToT (nanosec)	Coordinates	
Time of Arrival	Time over Threshold	X	Y
1.134267353184	425	144	140
1.134267353162	875	57	234
1.134267353137	875	235	149
1.134267353120	125	178	140
1.134267353111	975	5	130



In situ synchrotron x-ray diffraction studies monitoring mechanochemical reactions of hard materials: Challenges and limitations

Cite as: Rev. Sci. Instrum. 92, 114102 (2021); doi: 10.1063/5.0068627

Submitted: 26 August 2021 • Accepted: 26 October 2021 •

Published Online: 8 November 2021



Tobias Rathmann,¹  Hilke Petersen,¹ Steffen Reichle,¹ Wolfgang Schmidt,¹ Amol P. Amrute,¹ Martin Etter,² and Claudia Weidenthaler^{1,a)} 

AFFILIATIONS

¹ Max-Planck-Institut für Kohlenforschung, Heterogeneous Catalysis, Kaiser-Wilhelm-Platz 1, 45470 Mülheim, Germany

² Deutsches Elektronen Synchrotron (DESY) P02.1 PETRA III, Notkestr. 85, 22607 Hamburg, Germany

^{a)} Author to whom correspondence should be addressed: weidenthaler@mpi-muelheim.mpg.de

ABSTRACT

In situ monitoring of mechanochemical reactions of soft matter is feasible by synchrotron diffraction experiments. However, so far, reactions of hard materials in existing polymer milling vessels failed due to insufficient energy input. In this study, we present the development of a suitable setup for *in situ* diffraction experiments at a synchrotron facility. The mechanochemical transformation of boehmite, γ -AlOOH, to corundum, α -Al₂O₃, was chosen as a model system. The modifications of the mill's clamping system and the vessels themselves were investigated separately. Starting from a commercially available Retsch MM 400 shaker mill, the influence of the geometrical adaptation of the setup on the milling process was investigated. Simply extending the specimen holder proved to be not sufficient because changes in mechanical forces need to be accounted for in the construction of optimized extensions. Milling vessels that are suitable for diffraction experiments and also guarantee the required energy input as well as mechanical stability were developed. The vessels consist of a steel body and modular polymer/steel rings as x-ray transparent windows. In addition, the vessels are equipped with a gas inlet and outlet system that is connectable to a gas analytics setup. Based on the respective modifications, the transformation of boehmite to corundum could be observed in an optimized setup.

© 2021 Author(s). All article content, except where otherwise noted, is licensed under a Creative Commons Attribution (CC BY) license (<http://creativecommons.org/licenses/by/4.0/>). <https://doi.org/10.1063/5.0068627>

I. INTRODUCTION

During the last few decades, mechanochemistry has become a very promising alternative to conventional syntheses, especially concerning sustainability and environmental friendliness.¹ Conventional solid-state reactions often require harsh reaction conditions concerning temperature and/or pressure.^{2,3} In the solid state, reactions are driven by diffusion that takes place at surfaces, interfaces, and/or defects. Compared to reactions in liquids or gases, solid-state reactions are slow processes. To increase both reaction and diffusion rates to a suitable level, usually very high temperatures are necessary.² Another way to force solids to react is applying elevated pressures, which is often used in combination with elevated temperatures.² Transferring them into a liquid or gaseous phase before the reaction, on the other hand, may require hazardous

solvents or equipment for high-energy processing such as melting or vaporization.^{4,5} Mechanochemical syntheses provide alternative reaction routes, and thus, the direct mechanical treatment of the solids can lead to simplified and economic processes.^{4,5} Further benefits are the option to obtain metastable products⁵ or enable (*in situ*) mechanical activations of solid catalysts.^{6,7} Among various types of laboratory mills, the most common ones are shaker mills and planetary ball mills.⁶ The energy supply via milling leads to mechanochemical reactions, which may differ significantly from thermally activated reactions.^{6,8,9}

A possibility to obtain information on the processes taking place during a mechanochemical reaction is the implementation of *in situ* characterization methods. Promising methods that already found application in research are *in situ* x-ray powder diffraction (XRPD) and/or Raman spectroscopy. The XRPD data provide

information about the composition of the crystalline phases in the milled sample at a specific time. The identification of the phases helps establish reaction mechanisms. Moreover, Rietveld refinements of the diffraction data allow for the quantification of the crystalline phases. The calculated concentrations are used to identify the underlying kinetics of the reaction. The first successful application of *in situ* XRPD for a mechanochemical process was the monitoring of the synthesis of zeolitic imidazolate frameworks (ZIFs).¹⁰ The authors were able to investigate the influence of catalytic additives such as organic liquids or ionic species on the reaction. In addition, this was the first report on using a modified shaker mill for *in situ* XRPD experiments.¹⁰ The authors modified a commercial shaker mill in such a way that the mill could be mounted on a powder diffraction beamline at a synchrotron source. Two modifications were implemented:^{10,11} (a) the sample holder (clamping system) was extended to allow access to the incident x-ray beam and (b) the replacement of the original stainless steel jars by the transparent polymeric jars (Perspex). An example that illustrates well the benefits of *in situ* XRPD measurements compared to *ex situ* measurements is the monitoring of the formation of pharmaceutical co-crystals.^{11,12} Likewise, structural transformations taking place during milling reactions, which were unknown for a certain reaction before, are accessible via *in situ* XRPD. Examples are amorphization and recrystallization processes as shown for a ZIF in an aqueous environment.¹³ Thus, specially adapted milling jars should allow for investigation of further influences on the reaction process. An example is the use of thermally insulated milling vessels to explore the effect of temperature changes on the milling product. By this, it was possible to reveal a change in the mechanism at different temperatures during the formation of coordination polymers from CdCl₂ and cyanoguanidine.¹⁴

Until now, the majority of the published *in situ* studies investigated the syntheses of organic or metal-organic soft matter substances, such as metal-organic frameworks (MOF's) or organic co-crystals.^{10–20} The reactions of hard matter that are in the focus of our studies require different experimental setups though. To make *in situ* XRPD studies on such materials feasible, specific technical requirements must be fulfilled. Access to synchrotron radiation is mandatory because a high x-ray flux is required to ensure that the incident x-ray beam not only enters the jar but also that the diffracted beam could leave it again with sufficient intensity. On the other hand, also the adaptation of the milling setup is required to account for reactivity and safety.

Herein, we investigate several adaptations of a typical shaker mill (Retsch MM 400) required to allow for *in situ* XRPD measurements and their influence on the milling process of hard matter. Such reactions cannot be performed in polymer vessels but require milling vessels made from steel or comparable robust materials.^{21,22} As a model system, we have chosen the transformation of boehmite, γ -AlOOH, to corundum, α -Al₂O₃, which is one of the hardest known materials. The transformation has been studied previously as an example for the synthesis of high surface area α -Al₂O₃ by mechanochemistry.²³ The reaction was originally performed in a shaker mill in milling vessels made from tungsten carbide or steel to provide enough impact for a successful transformation. This study will highlight the impact of different modifications of a commercial ball mill both on the milling processes and the products.

II. EXPERIMENTS

A. Milling experiments and *ex situ* x-ray diffraction studies

In a recent publication, Amrute *et al.*²³ reported the successful transformation of boehmite (γ -AlOOH) to high surface area corundum (α -Al₂O₃), which was proven by *ex situ* XRPD. Before performing *in situ* XRPD experiments at a synchrotron beamline, preliminary tests were performed in our laboratory. The first experiment was performed with the original setup of a Retsch MM 400 shaker mill {original vessel mount, steel vessels with 25 ml volume, and two 15 mm stainless steel balls [Figs. 1(a) and SI1]} by milling 1 g γ -AlOOH (Sasol, DISPAL 11N7-80) for 120 min with a frequency of 25 Hz. *Ex situ* XRPD measurements were performed in-house on an STOE STADI P diffractometer in Debye-Scherrer geometry. Monochromatization of the molybdenum radiation (MoK α_1) was achieved with a curved germanium monochromator. For the measurements, the samples were filled in borosilicate capillaries with 0.5 mm inner diameter. Diffracted intensities were recorded with a DECTRIS Mythen 1K detector.

As revealed by the XRPD pattern in Fig. 2(a), the transformation of boehmite to corundum proceeds in accord with the published data. The main phase obtained is α -Al₂O₃, with some remaining boehmite as well as γ -Al₂O₃ and tohdite as by-products. Admixed iron was also observed in the sample as a result of the abrasion of the steel from the vessel and the milling balls.

A modified shaker mill setup for *in situ* milling experiments similar to the one reported by Halasz *et al.*¹¹ is available at the synchrotron P02.1 beamline at PETRA III [Deutsche Elektronen-Synchrotron (DESY), Hamburg, Fig. 1(b)]. The major change compared to the original commercial instrument is the application of extensions for positioning the milling vessels in the x-ray beam [Figs. 1(b) and 1(c)]. In this setup, the vessel holder is rotated by 90° and mounted on an extension that allows placing the milling vessel in the vessel holder on a position above the housing of the mill. In this position, the x-ray beam can pass directly through the milling vessel. The modified shaker mill was supposed to be then used for milling experiments with hard matter as reported by Amrute *et al.*²³

First, an *ex situ* experiment was performed to test the suitability of the extensions available at the synchrotron P02.1 beamline at PETRA III (DESY, Hamburg). The *ex situ* XRD data indicate a quite different product composition to the experiment without the extensions [Fig. 2(b)]. While this setup worked very well for the synthesis of soft matter,^{15,18,21,24,25} it failed to reproduce the transformation of the alumina as reported by Amrute *et al.*²³ The XRPD patterns in Figs. 2(a) and 2(b) show that the extensions significantly affect the milling process and the mechanochemical transformation. With the extensions, only minute amounts of α -Al₂O₃ are observed together with unreacted boehmite, γ -Al₂O₃, and tohdite. The different phase compositions show that using the extensions has a tremendous impact on the milling performance.

In the past, milling vessels entirely made from polymethyl methacrylate (PMMA) were used for *in situ* x-ray diffraction studies.^{10–20,24–28} Such polymer jars are not suitable for reacting the very hard alumina as addressed above. The transformation from boehmite to corundum requires a high energy input that cannot be achieved with polymer vessels, as we will discuss later in more

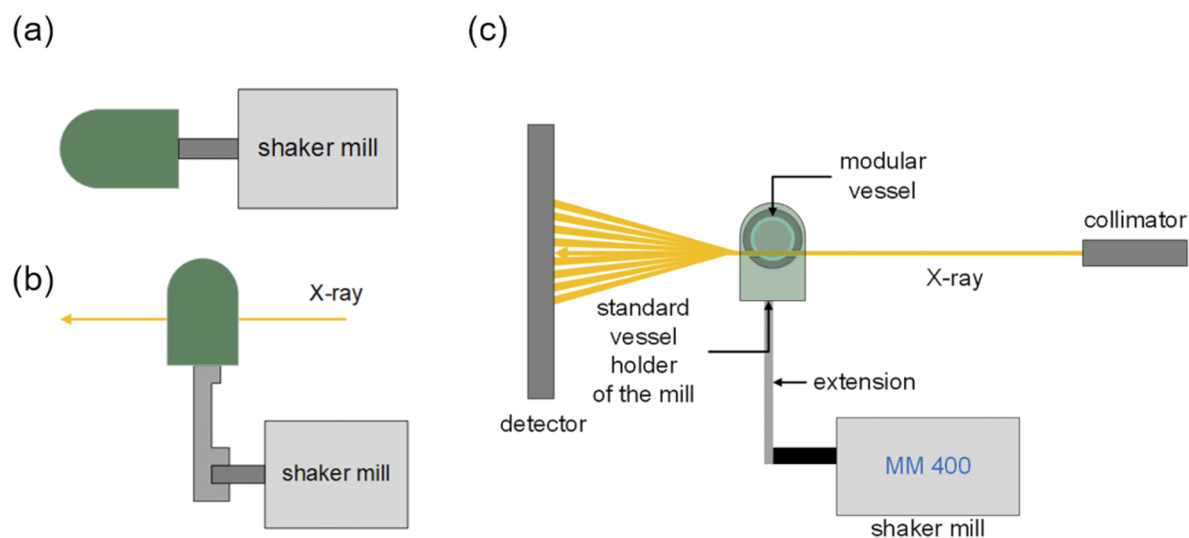


FIG. 1. Schematic diagrams of (a) an original unmodified Retsch MM 400 ball mill, (b) the modified MM 400 mill used in this study, and (c) the setup required for *in situ* x-ray diffraction experiments at the synchrotron.

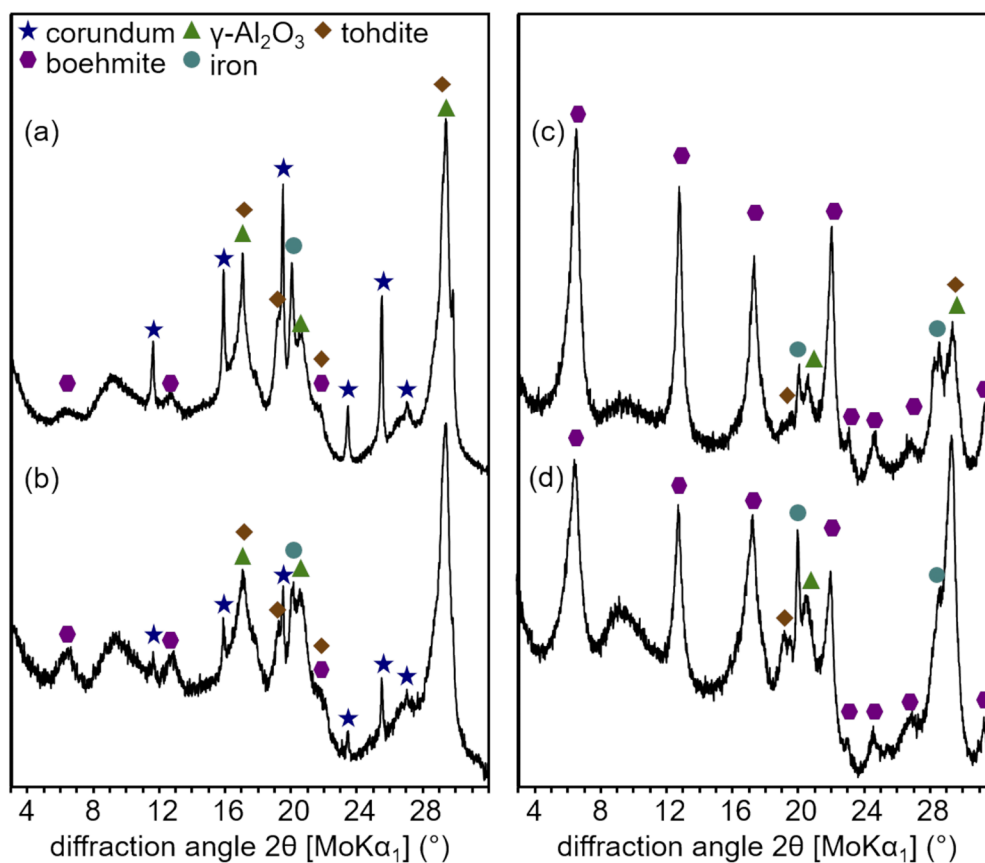


FIG. 2. *Ex situ* XRPD patterns of the products of ball milling γ -AlOOH for 120 min. (a) Milling performed with the original setup and (b) milling performed with a modified clamping system as available at P02.1 at PETRA III. *Ex situ* XRD patterns of the products obtained after milling γ -AlOOH for (c) 60 min and (d) 120 min with the original clamping system and modified stainless steel vessels with PMMA windows.

detail. Therefore, stainless steel milling vessels with two rectangular windows were constructed (further called vessel generation 1).⁹ The windows provide a free pathway for the incoming and diffracted x-ray beam. Figure 3(a) shows the first version, for which a removable polymeric ring (PMMA, modular vessel design) was inserted as an x-ray transparent window inside the jars. The ring covered more than 50% of the chamber surface. In a second preliminary in-house experiment, these milling vessels were tested for the same reaction reported above using the original Retsch clamping system. *Ex situ* XRD data reveal that after milling for 60 and 120 min, no transformation of boehmite to corundum took place [Figs. 2(c) and 2(d)]. Only a minor fraction of boehmite was converted to γ -Al₂O₃ and tohdite. The energy input in this modified milling vessel was not sufficient to complete the conversion of boehmite to corundum. However, the energy was sufficient to damage the polymer ring within the vessel [Fig. 3(b)].

These preliminary experiments thus revealed two obvious problems:

- First, the extensions used for the *in situ* XRD experiment seem to not allow for the same energy transfer as the original clamping system for the milling vessels.
- Second, the stainless steel milling vessels with the polymer rings do not allow for the same reaction as the original stainless steel vessels provided by Retsch.

We, therefore, investigated the reasons for the failure in some more detail to come up with solutions for both problems.

B. Redesign of the extensions for the vessel mount

The shaker mill transfers kinetic energy to the grinding media by generating an oscillating movement of the vessels. At every contact between the ball and vessel, an exchange of momentum takes place. This collision-driven principle leads to the high impact-to-friction ratio that is characteristic for shaker mills. The momentum of an object is proportional to its mass and velocity. Since the vessel is securely mounted on the holder, the oscillating weight results from the sum of all parts firmly attached to the vessel holder. The type of movement has an important influence. The oscillating mass does not perform the oscillation on a horizontal trajectory. Instead, based

on the mill design, the oscillation proceeds on a small circle segment [Fig. SI2(a)]. During milling, every part of the oscillating mass performs a motion on this circle segment. Characteristic for such motions is that the mean velocity of the moving objects is directly proportional to the radius of the corresponding circle. Inspection of the mill with the extensions used for our experiments as well as for others^{15,18,21,24,25} reveals that the radius is reduced by about 30% if the original clamping system is replaced by the one with the extensions (Figs. SI3 and SI4). This corresponds to the same decrease in the average velocity of the jars. Since the mean kinetic energy of the vessel is proportional to the square of the mean velocity, the mean kinetic energy reduces approximately to 50% compared to the original setup. Consequently, new extensions were developed, which bring the vessels to the same radial positions as in the original system.

Another important point we considered for their construction is the mechanical stability of the extensions. For the mill used in this study, accelerations up to a g-factor of 36 are possible.²⁹ This results in high centrifugal forces on the moving components that may cause deformations of the extensions (Fig. SI5). Therefore, the extensions have to provide high mechanical stability. At the same time, their weight must be minimized to keep the total moving mass as low as possible to not damage the mechanics of the shaker mill and to prevent unwanted tilting (Fig. SI5). Furthermore, the total mass should be distributed in a way that mass reduction is achieved at parts with a greater lever to the mill's inner mechanics (torque reduction).

Compared to the extensions provided at P02.1 (PETRA III, Hamburg) [Fig. 4(a)], the following major changes were made to the new extensions [Fig. 4(b)] to comply with the requirements discussed above:

- To reduce weight, the material of the redesigned extensions was changed from steel to aluminum.
- The average thickness of the upright part was increased compared to the original extensions. To ensure the required distance between the mill and the remounted clamp, the profile was changed to a more inclined shape [Figs. 4(c) and 4(d)].
- The width of the extensions was reduced to fit exactly to the connection parts of the mill [Fig. 4(c)].

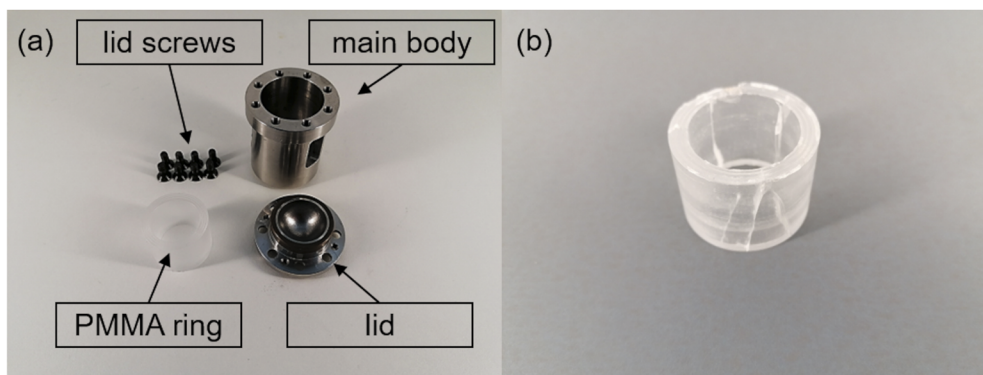


FIG. 3. (a) Demounted x-ray transparent stainless steel milling vessel with a PMMA ring covering the windows in the steel housing (vessel generation 1)⁹ and (b) the PMMA ring after usage.

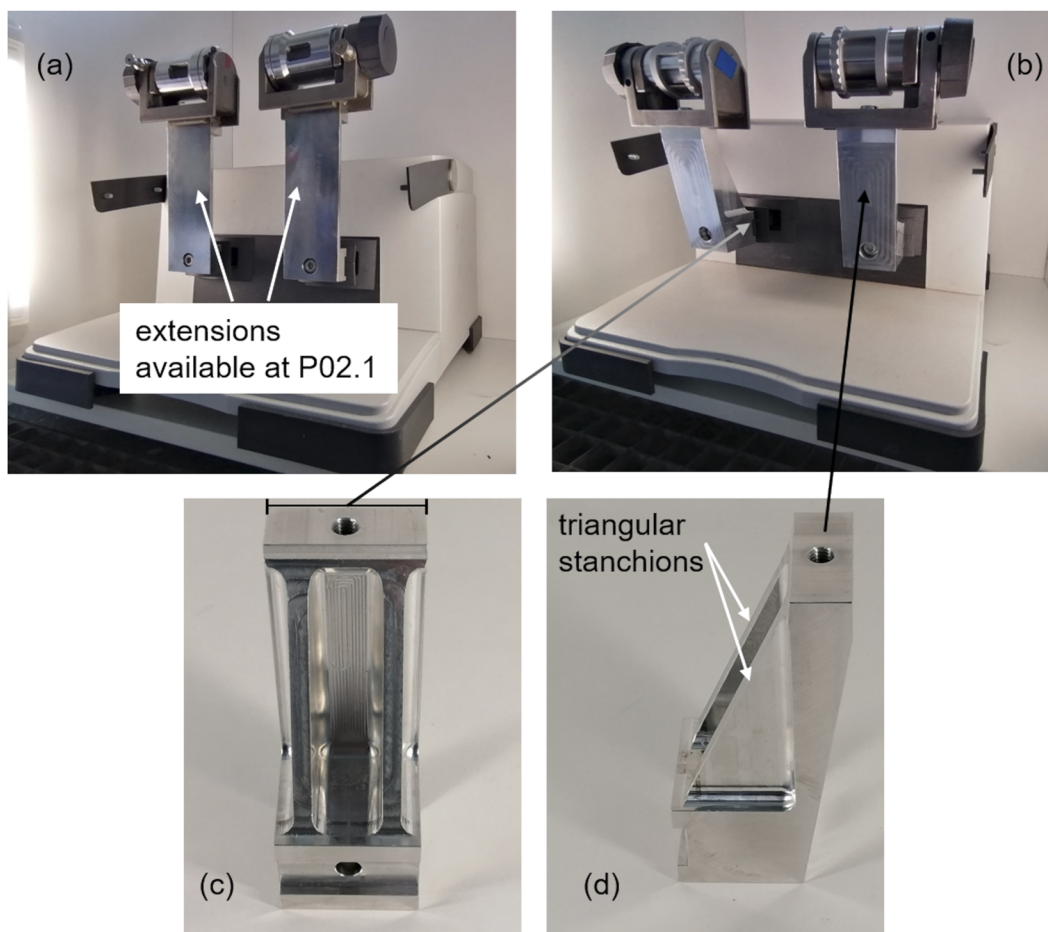


FIG. 4. Photographs of the Retsch MM 400 with (a) the original extensions available at P02.1 at PETRA III and (b) the newly designed extensions made from aluminum. (c) Front view of the extension and (d) side view showing the triangular stanchions.

- To increase the stability, the central extension part is supported by two triangular stanchions [Fig. 4(d)].

C. Mechanical considerations for the design of the milling vessels suitable for *in situ* x-ray experiments

The use of steel milling vessels with a polymeric ring as an x-ray transparent window failed to reproduce the conversion of boehmite to corundum as reported above. More than 50% of the inner vessel surface consists of polymer that affects the overall mechanical properties significantly. The energy transfer from the grinding media (balls) toward the powder is mainly depending on an interaction between the balls, the powder, and the walls of the vessel. The two main properties of the wall material that affect the energy transferred in the mechanochemical process are the elastic modulus²¹ and the hardness.²² While the elastic modulus specifies the resistance of the material against the elastic deformation, the hardness defines the resistance against the penetration by another solid object. Preliminary considerations about the factors governing the

respective forces are discussed in the [supplementary material](#) (see also Fig. SI6). Another important factor is that the movement of the balls is affected by the vessel materials. Regarding the lack of transformation of boehmite to α - Al_2O_3 in the presence of PMMA walls and the different mechanical properties of steel and polymer, we expect that the balls are slowed down during collisions with the PMMA wall. This would result in a decrease in their kinetic energy and thus lead to reduced forces exerted on the powder during the next collision. A material depending quantity that could give information about this is the coefficient of restitution. The coefficient of restitution describes how elastic or inelastic a collision takes place and is calculated from the ratio between the ball velocities perpendicular to the contact surface after and before the collision. For an ideal elastic collision, the coefficient of restitution would be 1, while it would be 0 for a complete inelastic one. However, the coefficient of restitution is also depending on other factors besides the vessel materials. These factors include the geometry and, to a limited degree, the velocity of the colliding objects. Unfortunately, we could not determine the mean velocities of the balls for our conditions. Furthermore, the powder layer inside the vessel has an additional

influence. Simulating this is challenging since the powder properties are not constant over the milling process. For free-flowing steel powder, a strong decrease in the coefficient of restitution is reported for increasing powder thicknesses in the range from 0 to 2 mm.³⁰ Last but not least, structural features of the milling vessels may also influence the collision behavior. These include a small free space between the ring and the vessel wall that is necessary to put the ring inside the vessel or the fixation of the ring by contact pressure horizontal to the impact surface. Determination of the coefficient of restitution while taking all these influences into account would allow a quantitative statement about the effect on the ball movement. However, due to these numerous influences and the complexity to integrate them into a suitable experimental setup, this exceeds the scope of this publication. In summary of all the above considerations, a reduction of the polymer surface within the milling vessels is highly advisable.

D. Decomposition of the polymeric parts of vessel generation 1

As shown above, another problem of the polymeric rings used in vessel generation 1 is their tendency to break during milling [Fig. 3(b)]. *In situ* gas flow investigations performed during ball milling in respective milling vessels show that the polymer does not only break but also decompose. Since these vessels were also designed for catalyzed reactions including gas flows (with gas in- and outlet), the decomposition of the polymer could be monitored by analyzing the outlet gas. To analyze the gas phase inside the milling vessel, *in situ* infrared (IR) spectroscopy measurements were performed with a Thermo Nicolet Avatar 370 FTIR spectrometer. The spectrometer was connected via a gas capillary to the milling vessel. During milling using an empty vessel with a 15 mm stainless steel ball, a continuous argon gas flow of 20 ml min⁻¹ was applied to transport the gas atmosphere from the vessel to the IR spectrometer. Before the experiments, the IR instrument was flushed with an argon flow of 10 ml min⁻¹ overnight and of 20 ml min⁻¹ for 1 h at a chamber temperature of 80 °C. To flush the vessel, an argon flow of 20 ml min⁻¹ was applied for 30 min each at complete rest and a very low milling frequency of 3 Hz. The IR spectroscopy was equipped with a DTGS detector with a resolution of 4 cm⁻¹. The spectral range was 650–4000 cm⁻¹. For further analysis of the gas atmosphere in the milling vessel, a Balzers ThermoStar mass spectrometer (MS) was connected with a gas capillary to the gas outlet of the IR spectrometer. The instrument was equipped with a QME 200 analyzer (Pfeiffer).

As a blind experiment, an empty steel vessel without any polymer parts was connected to the gas detection system and milling was performed for 60 min at 25 Hz [Fig. 5(a)]. The vessel was flushed continuously with argon. The IR spectra indicate the presence of CO₂ and H₂O from the atmosphere inside the vessel and the tubing lines.³¹ In addition, small bands of hydrocarbons (–CH₃) are also visible in the spectra. The hydrocarbon is likely residual oil from the machining of the steel vessels.

The IR spectra obtained from the milling vessel generation 1, whose inner surface is covered with more than 50% PMMA, show already after 5 min an increase in the intensity of CO₂ [Fig. 5(b)].³¹ In addition to the CO₂ bands, the appearance of additional IR modes is detected. The modes in the spectral range from 3000

to 2900 cm⁻¹ can be assigned to hydrocarbons (sp³-hybridized). In the spectral range from 1750 to 1735 cm⁻¹, vibrational modes of ester groups and from 1140 to 1240 cm⁻¹ stretching vibration of keto groups appear.³² These modes are typical for the methyl methacrylate, the monomer PMMA is formed of.³² This product is the main product of the thermal decomposition of PMMA at 493–503 K. MS data also reveal a significant increase in the signals corresponding to the decomposition products CO₂ (44 u), CO (28 u), and H₂O (18 u) already after 3 min of milling [Fig. SI7(a)]. For this reason, the contact of the x-ray transparent window material with the balls should be either avoided or at least reduced to a minimum.

E. Design of vessel generation 2

To address this problem in the second generation of modified milling vessels, two rectangular windows were cut into the walls of the stainless steel vessels. The cutouts were closed with two polymer plates fixed by screws (Fig. 6). The window size should be large enough to not cut the beam. The motion of the jars on a small circle segment determines the needed width of the windows [Figs. SI2(a) and SI2(b)]. If the length of the covered path ΔU and the construction-related radius r of this motion are known, the angle γ between the points of maximum vessel deflection can be determined. As displayed in Fig. SI2(a), r and γ define the horizontal distance s that the vessel covers between the central position and maximum deflection.

Milling with vessel generation 2 resulted in the detection of small amounts of CO₂, H₂O, and hydrocarbons as for the full steel reaction vessel [Fig. 5(c)].³¹ However, no decomposition products from PMMA could be detected.

With a modified setup equipped with an intermediate development stage of new extensions and the modified second generation milling vessels, *in situ* synchrotron diffraction experiments were performed. The measurements were performed at the Powder Diffraction and Total Scattering Beamline P02.1 at PETRA III (DESY, Hamburg). The wavelength of the x rays was 0.207 Å, and a PerkinElmer XRD1621 area detector was used for data acquisition with a recording time of 10 seconds per frame. Data integration from the measured frames was performed with the DAWN software.³³

An XRD pattern taken directly after switching on the ball mill displays the reflections of boehmite and the broad scattering contribution from the PMMA windows between 1 and 3° 2 θ (Fig. 7). However, after milling for 20 min, the intensities of the reflections are weak, and after 60 min, no reflections from the sample are visible anymore. Two factors are likely to be responsible for this in combination. On the one hand, the distribution of the sample inside the vessel changes during the milling process. At the beginning of the process, the sample is a free-flowing powder. During milling, the powder starts to coat the walls of the vessel and only a small amount remains as a free-flowing powder. On the other hand, the small gap between the polymer window and the jar body [Fig. 6(a)] has two drawbacks:

- (a) It hinders the powder to stick to most of the central surface of the x-ray transparent window and also no accumulation of free-flowing powder takes place there. Therefore, the x-ray beam cannot interact with larger volume fractions of the powder, resulting in reflections with very low intensity.

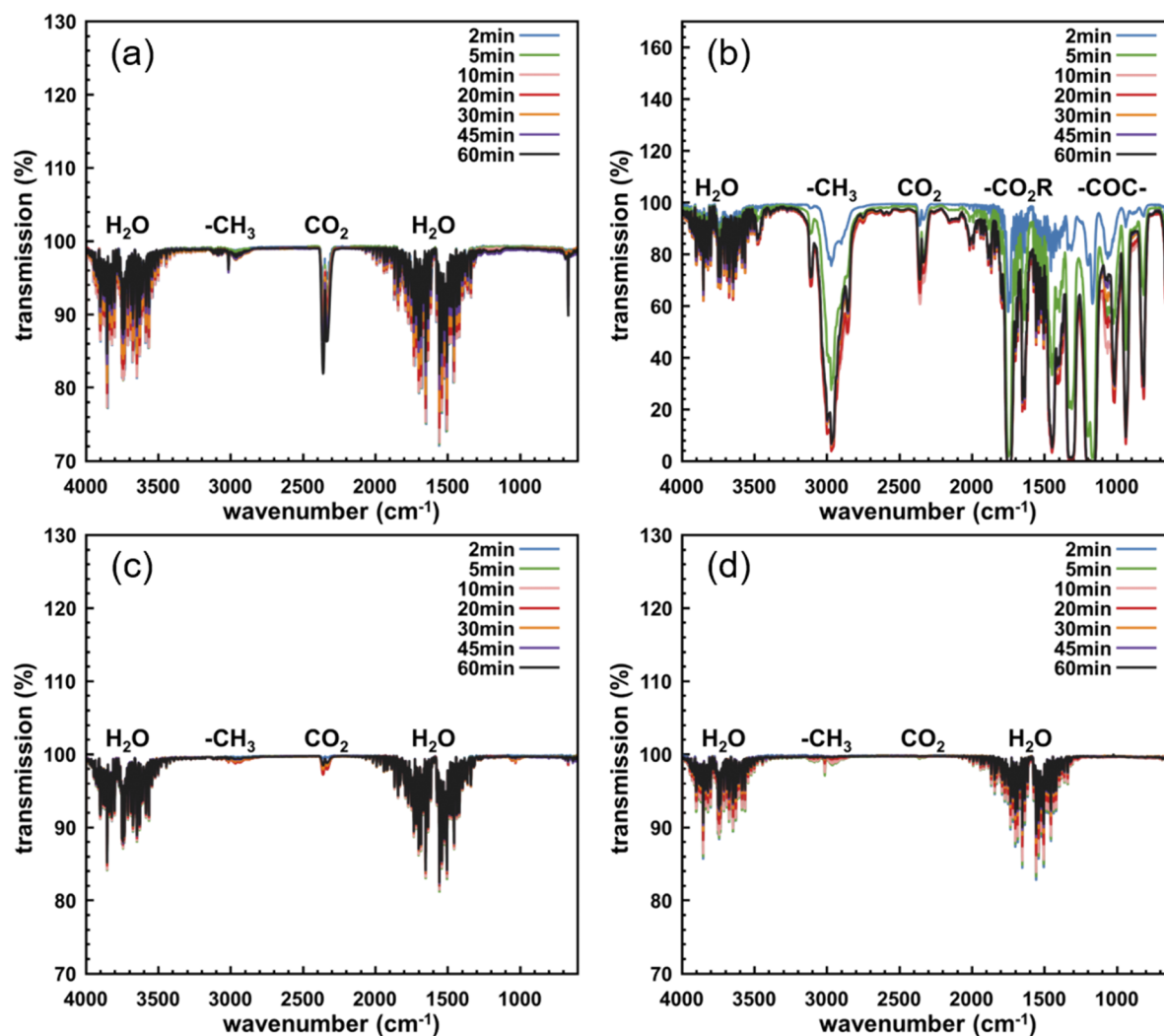


FIG. 5. IR spectra of the gas phase inside the milling vessels obtained *in situ* during milling with one stainless steel ball of 15 mm diameter in the empty vessels. (a) Vessel with a full steel milling chamber as reference. (b) First generation vessel with the PMMA ring. (c) Second generation vessel with two cutouts in the stainless steel body covered with PMMA. (d) Third generation vessel with the PMMA ring and inner steel ring.

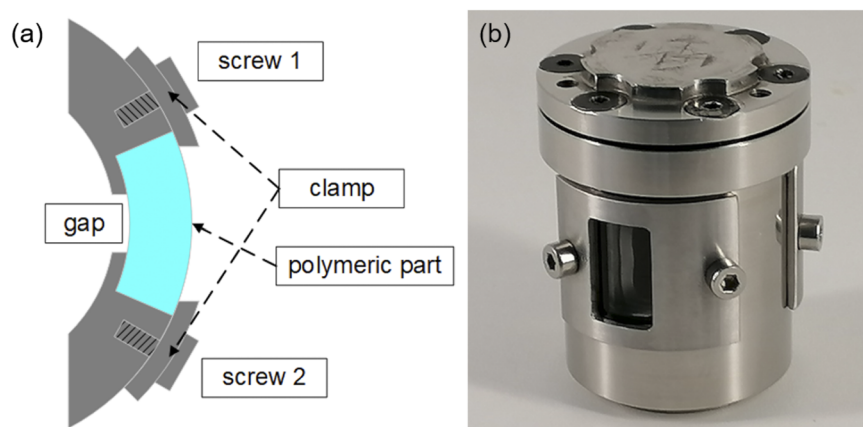


FIG. 6. Vessel generation 2: (a) schematic diagram of the side profile of the redesigned window and (b) picture of a complete mounted vessel with the updated window design.

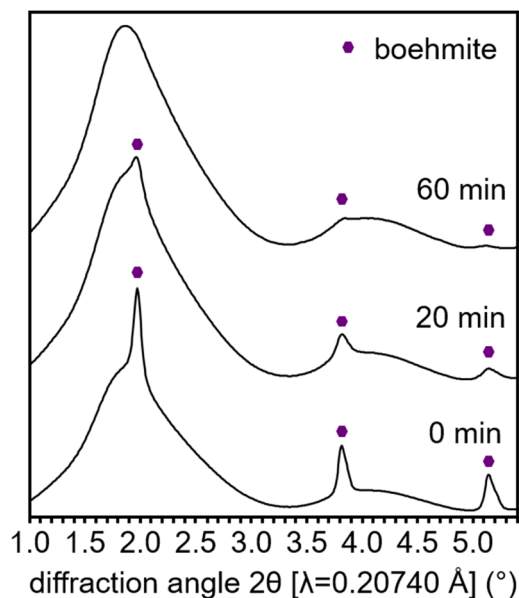


FIG. 7. *In situ* x-ray diffraction patterns of ball milled boehmite measured after different milling times. The used setup comprises the modified second generation vessels and an intermediate stage of new extensions.

- (b) Powder that gets trapped at the edges of the gap between the polymer and the steel would not be effectively milled because it does not get into contact with the 15 mm balls. Thus, diffraction data obtained from this powder would not represent the overall vessel content.

F. Design of vessel generation 3

For this reason, the vessel design had to be changed once more. For vessel generation 3, the design was changed back to a PMMA ring covering the cutouts from the inside. An additional inner metal ring with a wall thickness of 500 μm (Fig. 8) covers the PMMA ring. No decomposition products of PMMA have been observed, proving that the metal ring protects the polymer [Figs. 5(d) and SI7(b)].

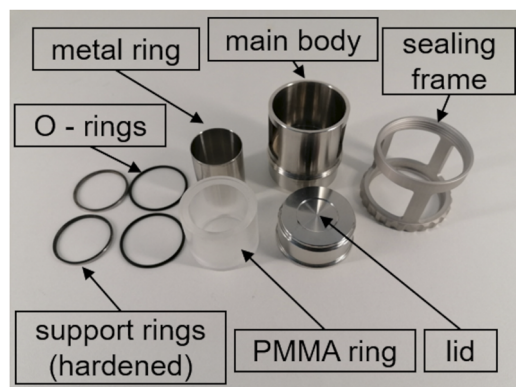


FIG. 8. Photograph of the disassembled third generation milling vessel with the labeled single components.

However, the stabilization comes at the expense of the diffracted x-ray intensity due to the absorption by the inner metal ring. In addition, depending on the type of metal used for the ring, additional reflections may appear in the powder pattern. Figure 9 summarizes the *in situ* XRD patterns for different vessel modifications. Figure 9(a) shows the XRD pattern obtained from the empty vessel with the PMMA ring and the stainless steel balls with broad scattering contribution from the polymer and the steel peaks. If aluminum is used for the metallic ring, intense reflections from the aluminum are visible in the XRD pattern already after 10 s data collection time per frame [Fig. 9(b)]. If a steel ring is used, the steel peaks become very prominent [Fig. 9(c)]. All peaks are split because diffraction occurs at different positions inside the jar coming from both walls and the balls. The recording time per frame was increased to 60 s to obtain higher intensities of the alumina reflections.

After all these modifications had been developed, the final experiment was performed at the beamline P02.1. The vessel shown in Fig. 9 was used for milling 1 g boehmite (Fig. SI9) at 25 Hz with two 15 mm stainless steel balls. Finally, after the successive modification of extensions and vessels, the successful transformation of boehmite to $\alpha\text{-Al}_2\text{O}_3$ could be monitored by *in situ* XRD (Fig. SI10). The powder patterns show a high scattering background caused by the vessel and the balls. However, the background obtained from an empty vessel with balls can be subtracted, resulting in the *in situ* XRD patterns reflecting the transformation of boehmite to corundum (Fig. 10).

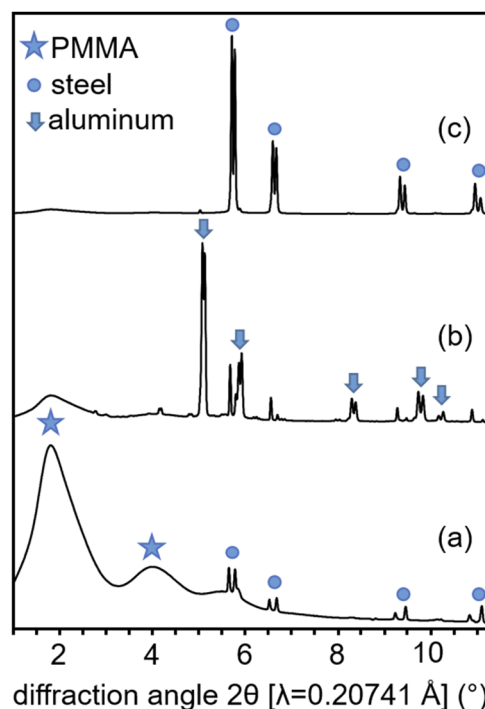


FIG. 9. *In situ* x-ray diffraction patterns obtained from (a) an empty vessel with a PMMA window and steel balls (generations 1 and 2), (b) an empty vessel with a PMMA and an aluminum ring and steel balls (generation 3), and (c) an empty vessel with a PMMA and a steel ring and steel balls (generation 3).

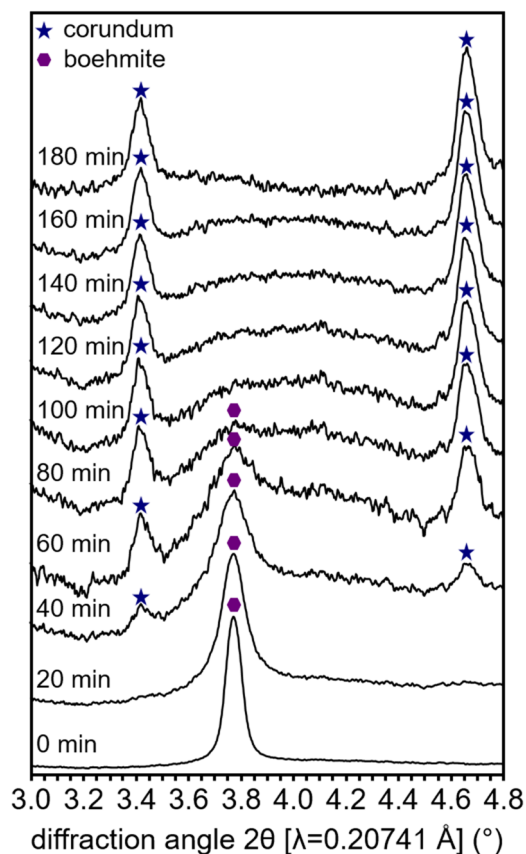


FIG. 10. *In situ* x-ray diffraction patterns of ball milled boehmite were collected after different times of milling. The used setup comprises the third generation vessels with an additional steel ring and the new aluminum extensions. The pattern obtained from an empty vessel with balls was multiplied with a weighting factor and subtracted from the experimental data. For the period between 0 and 160 min, the weighting factor is 0.8, and for 180 min, it is 0.6. The reason for the varying weighting factor is the fluctuation of the incident beam intensity.

III. CONCLUSION AND OUTLOOK

Monitoring the mechanochemical reactions by x-ray diffraction experiments within a ball mill is a very challenging task. While it is possible to mount a shaker mill on a synchrotron beamline, the technical modifications to place the milling vessels in the x-ray beam and the additional modifications to the vessels themselves have proven to be extremely complex. The investigations have shown that it is not possible to simply extend the specimen holder extensions but that it is necessary to take into account the change in mechanical forces that may occur. The influence on the mechanical forces can be so great that solid-state reactions of hard matter can sometimes no longer proceed successfully. For this reason, the various influences that technical changes to the original setup of a shaker mill can have on the products formed were systematically investigated. In addition to the possible change in force input, the influence of changes in the vessels was investigated. For various reactions of hard materials, x-ray transparent polymer (e.g., PMMA) grinding vessels cannot be used. Our investigations have shown that it is necessary

to use steel vessels that must nevertheless be equipped with x-ray transparent windows. Polymers decompose due to the mechanical stress during grinding. This was successfully prevented by developing a modular window made of a polymer and a metal ring. Based on these developments, the conversion of boehmite to corundum could be successfully followed by *in situ* synchrotron x-ray diffraction experiments.

In further studies, new composite materials are being searched for as the window material by which the number of unwanted reflections of the window itself can be reduced. In addition, gas phase reactions are planned that will enable *operando* x-ray diffraction experiments during mechanocatalysis.

SUPPLEMENTARY MATERIAL

See the [supplementary material](#) for photographs of the modified mill, extensions, and vessels and schematic diagrams describing geometric details and dimensions as well as MS data and x-ray powder diffraction data.

ACKNOWLEDGMENTS

We acknowledge DESY (Hamburg, Germany), a member of the Helmholtz Association HGF, for the provision of experimental facilities. Parts of this research were carried out at PETRA III, beamline P02.1. We thank Jan Ternieden, Priyanka Sharma, and Isabella Kappel for their support during the synchrotron measurements. The workshop of the MPI is gratefully acknowledged for the construction of all the redesigned components.

AUTHOR DECLARATIONS

Conflicts of Interest

The authors have no conflicts to disclose.

Author Contributions

C.W. and W.S. conceived the project. T.R., H.P., and S.R. developed the hardware modifications on the mill and the vessel. They planned and performed all *ex situ* and *in situ* experiments. A.P.A. supported the *ex situ* milling experiments on boehmite. M.E. was the beamline scientist supporting the experimental setup at PETRA III. The manuscript was written by T.R., W.S., and C.W. with input from all authors.

DATA AVAILABILITY

The data that support the findings of this study are available from the corresponding author upon reasonable request.

REFERENCES

- ¹T. Friščić, C. Mottillo, and H. M. Titi, *Angew. Chem., Int. Ed. Engl.* **59**, 1018 (2020).
- ²L. Smart and E. A. Moore, *Solid State Chemistry: An Introduction* (Taylor & Francis, Boca Raton, 2005).
- ³R. Dronskowski, S. Kikkawa, and A. Stein, *Handbook of Solid State Chemistry* (Wiley, Hoboken, 2017).
- ⁴V. V. Boldyrev, *Mater. Sci. Forum* **225–227**, 511 (1996).
- ⁵V. V. Boldyrev and K. Tkáčová, *J. Mater. Synth. Process.* **8**, 121 (2000).

- ⁶P. Baláž, M. Achimovičová, M. Baláž, P. Billik, Z. Cherkezova-Zheleva, J. M. Criado, F. Delogu, E. Dutková, E. Gaffet, F. J. Gotor, R. Kumar, I. Mitov, T. Rojac, M. Senna, A. Streletsii, and K. Wiczorek-Ciurowa, *Chem. Soc. Rev.* **42**, 7571 (2013).
- ⁷S. Immohr, M. Felderhoff, C. Weidenthaler, and F. Schüth, *Angew. Chem., Int. Ed.* **52**, 12688 (2013).
- ⁸V. V. Boldyrev and E. G. Avvakumov, *Russ. Chem. Rev.* **40**, 847 (1971).
- ⁹H. Petersen, S. Reichle, S. Leiting, P. Losch, W. Kersten, T. Rathmann, J. Tseng, M. Etter, W. Schmidt, and C. Weidenthaler, *Chem. Eur. J.* **27**, 12558 (2021).
- ¹⁰T. Friščić, I. Halasz, P. J. Beldon, A. M. Belenguer, F. Adams, S. A. J. Kimber, V. Honkimäki, and R. E. Dinnebier, *Nat. Chem.* **5**, 145 (2013).
- ¹¹I. Halasz, S. A. J. Kimber, P. J. Beldon, A. M. Belenguer, F. Adams, V. Honkimäki, R. C. Nightingale, R. E. Dinnebier, and T. Friščić, *Nat. Protoc.* **8**, 1718 (2013).
- ¹²I. Halasz, A. Puškarić, S. A. J. Kimber, P. J. Beldon, A. M. Belenguer, F. Adams, V. Honkimäki, R. E. Dinnebier, B. Patel, W. Jones, V. Štrukil, and T. Friščić, *Angew. Chem., Int. Ed. Engl.* **52**, 11538 (2013).
- ¹³A. D. Katsenis, A. Puškarić, V. Štrukil, C. Mottillo, P. A. Julien, K. Užarević, M.-H. Pham, T.-O. Do, S. A. J. Kimber, P. Lazić, O. Magdysyuk, R. E. Dinnebier, I. Halasz, and T. Friščić, *Nat. Commun.* **6**, 6662 (2015).
- ¹⁴K. Užarević, V. Štrukil, C. Mottillo, P. A. Julien, A. Puškarić, T. Friščić, and I. Halasz, *Cryst. Growth Des.* **16**, 2342 (2016).
- ¹⁵P. A. Julien, K. Užarević, A. D. Katsenis, S. A. J. Kimber, T. Wang, O. K. Farha, Y. Zhang, J. Casaban, L. S. Germann, M. Etter, R. E. Dinnebier, S. L. James, I. Halasz, and T. Friščić, *J. Am. Chem. Soc.* **138**, 2929 (2016).
- ¹⁶T. Stolar, L. Batzdorf, S. Lukin, D. Žilić, C. Mottillo, T. Friščić, F. Emmerling, I. Halasz, and K. Užarević, *Inorg. Chem.* **56**, 6599 (2017).
- ¹⁷H. Kulla, S. Haferkamp, I. Akhmetova, M. Röllig, C. Maierhofer, K. Rademann, and F. Emmerling, *Angew. Chem., Int. Ed. Engl.* **57**, 5930 (2018).
- ¹⁸P. A. Julien, L. S. Germann, H. M. Titi, M. Etter, R. E. Dinnebier, L. Sharma, J. Baltrusaitis, and T. Friščić, *Chem. Sci.* **11**, 2350 (2020).
- ¹⁹I. Halasz, T. Friščić, S. A. J. Kimber, K. Užarević, A. Puškarić, C. Mottillo, P. Julien, V. Štrukil, V. Honkimäki, and R. E. Dinnebier, *Faraday Discuss.* **170**, 203 (2014).
- ²⁰K. Užarević, I. Halasz, and T. Friščić, *J. Phys. Chem. Lett.* **6**, 4129 (2015).
- ²¹L. S. Germann, M. Arhangelskis, M. Etter, R. E. Dinnebier, and T. Friščić, *Chem. Sci.* **11**, 10092 (2020).
- ²²J. M. Andersen and J. Mack, *Chem. Sci.* **8**, 5447 (2017).
- ²³A. P. Amrute, Z. Łodziana, H. Schreyer, C. Weidenthaler, and F. Schüth, *Science* **366**, 485 (2019).
- ²⁴C. G. Vogt, S. Grätz, S. Lukin, I. Halasz, M. Etter, J. D. Evans, and L. Borchardt, *Angew. Chem., Int. Ed. Engl.* **58**, 18942 (2019).
- ²⁵L. Catalano, L. S. Germann, P. A. Julien, M. Arhangelskis, I. Halasz, K. Užarević, M. Etter, R. E. Dinnebier, M. Ursini, M. Cametti, J. Martí-Rujas, T. Friščić, P. Metrangolo, G. Resnati, and G. Terraneo, *Chem* **7**, 146 (2021).
- ²⁶A. A. L. Michalchuk, I. A. Tumanov, S. Konar, S. A. J. Kimber, C. R. Pulham, and E. V. Boldyreva, *Adv. Sci.* **4**, 1700132 (2017).
- ²⁷H. Kulla, F. Fischer, S. Benemann, K. Rademann, and F. Emmerling, *CrystEngComm* **19**, 3902 (2017).
- ²⁸S. Haferkamp, F. Fischer, W. Kraus, and F. Emmerling, *Beilstein J. Org. Chem.* **13**, 2010 (2017).
- ²⁹L. Borchardt and S. Grätz, *Handbuch Chemische Reaktoren*, edited by W. Reschetilowski (Springer Spektrum, Berlin, Heidelberg, 2020).
- ³⁰H. Huang, M. P. Dallimore, J. Pan, and P. G. McCormick, *Mater. Sci. Eng., A* **241**, 38 (1998).
- ³¹*NIST Chemistry WebBook*, NIST Standard Reference Database No. 69, edited by P. J. Linstrom and W. G. Mallard (National Institute of Standards and Technology, Gaithersburg, MD, 2018).
- ³²D. Sugumaran and K. J. Abd Karim, *eProc. Chem.* **2**, 1 (2017).
- ³³J. Filik, A. W. Ashton, P. C. Y. Chang, P. A. Chater, S. J. Day, M. Drakopoulos, M. W. Gerring, M. L. Hart, O. V. Magdysyuk, S. Michalik, A. Smith, C. C. Tang, N. J. Terrill, M. T. Wharmby, and H. Wilhelm, *J. Appl. Crystallogr.* **50**, 959 (2017).